Article

Mixed Phase-Incompatible Monolayers: Toward Nanoscale Anti-adhesive Coatings

Siwakorn Sakunkaewkasem, Maria D. Marquez, Han Ju Lee, and T. Randall Lee*

Cite This: *ACS Appl. Nano Mater.* 2020, 3, 4091−4101

Read Online

ACCESS | Metrics & More | Article Recommendations | SI Supporting Information

ABSTRACT: This article examines the interfacial properties of phase-incompatible self-assembled monolayer (SAM) films derived from the adsorption of mixtures of bidentate alkanedithiols terminated with oligo(ethylene glycol) and perfluorocarbon tailgroups. Precise control of the composition of the surface was achieved by adjusting the mole fraction of the adsorbates in the developing solution, leading to the ability to tune the interfacial composition and properties. The key driving force for the mixing of the phase-incompatible adsorbates is the strong "chelate" binding of the bidentate headgroup to the surface of gold. To elucidate this phenomenon, SAMs generated from the analogous monodentate adsorbates were studied alongside those generated from the bidentate adsorbates. Characterization of the SAMs generated from the bidentate adsorbates revealed a 1:3 volume ratio of THF:EtOH solution as the optimal solvent for the generation of SAMs in which both sulfur atoms of the bidentate oligo(ethylene glycol) and perfluorocarbon adsorbates were predominantly bound to the surface of gold. All SAMs were characterized by ellipsometry, contact angle goniometry, X-ray photoelectron spectroscopy, and polarization modulation infrared reflection−absorption spectroscopy. These characterizations revealed the ability to generate films with mixed phase-incompatible groups in which the mole fraction of the adsorbates on the surface mirror those present in the developing solutions, opening up an avenue toward the creation of interfaces not found in nature, with potential use as nanoscale anti-adhesive coatings.

KEYWORDS: self-assembled monolayer films, chelate binding, nanoscale, anti-adhesive coatings, mixed phase incompatibility
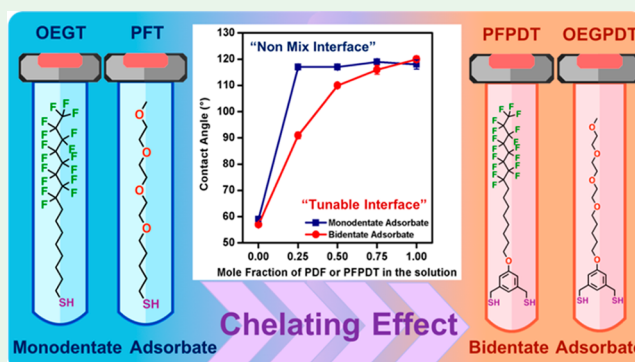

INTRODUCTION

The ability to manipulate the interfacial properties of solid materials has gained significant interest and has been the subject of extensive studies over the past two decades involving crucial applications, such as anticorrosion,[1−3] anti-adhesion,[4−7] antifouling,[8] and microfabrication technologies.[9−15] Several techniques have been developed to tune the interfacial properties of surfaces, among them, self-assembled monolayers (SAMs) are considered a simple and reliable system for modifying substrates of interest. Through chemical modification of the adsorbate, specific properties can be easily imparted onto surfaces. The incorporation of specific functional groups onto the adsorbates has been used as a means to control the interfacial properties of materials. Of particular interest have been partially fluorinated moieties, for their hydrophobicity and oleophobicity,[16,17] as well as polar groups such as oligo(ethylene glycol), for their ability to resist protein adsorption.[18−24] Our efforts seek to generate and study interfaces comprised of these two phase-incompatible species with the goal of developing next-generation antifouling coatings.

Studies of SAMs generated from partially fluorinated adsorbates have demonstrated that the wettability varies systematically with the degree of fluorination.[16] For example, SAMs derived from minimally fluorinated adsorbates, CF_3-terminated alkanethiols, exhibit higher wetting with polar liquids when compared to analogous *n*-alkanethiol SAMs, due to the presence of an oriented dipole in the former.[25] By increasing the number of fluorocarbons, the resulting SAMs become less wettable and more hydrophobic than the analogous *n*-alkanethiol SAMs.[26] The hydrophobicity and oleophobicity exhibited by fluorocarbon-based interfaces have led to further exploration of the wettability of partially fluorinated SAMs by Colorado and Lee,[27] patterning on indium tin oxide surfaces by Luscombe et al.,[28] and the generation of selective molecular transportation by Velleman et
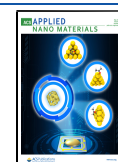
al.[29] Likewise, oligo(ethylene glycol)-based SAMs have been investigated for their hydrophilicity and ability to resist protein adsorption.[30] These fundamental observations have led to the use of oligo(ethylene glycol) films in several applications, including the inhibition of biomass adhesion,[31−33] biosensors,[34,35] control of cell adhesion,[36] and transistors.[37]

SAMs generated from a mixture of adsorbates bearing distinct functional groups have been used to tailor the interfacial properties of materials,[38] where most studies have utilized monodentate adsorbates.[32,39−42] There are, however, three major shortcomings of this approach: (1) preferential adsorption of one adsorbate over the other, (2) phase separation of disparate species on the surface, and (3) inconsistencies between adsorbate concentration on the surface and in solution.[39,42−44] Moreover, SAMs generated from monodentate adsorbates are less stable, chemically and thermally, than SAMs generated from bidentate adsorbates.[45]

Recent advances toward the generation of mixed interfaces saw the use of adsorbates bearing two chemically distinct functional groups within a single molecule; specifically, oligo(ethylene glycol) and alkyl tailgroups as well as a perfluoroalkyl and alkyl tailgroups.[46−48] SAMs generated from the aforementioned adsorbates exhibited interfacial properties that fall between those of the individual components. However, the use of such adsorbates is limited to a fixed 1:1 ratio of chemical functionalities, restricting the ability to fine-tune the interfacial properties. Moreover, the combination of certain functional groups, for example, fluorocarbons, considered to be hydrophobic,[49] and ethylene glycol moieties, highly hydrophilic,[46] onto the same adsorbate presents synthetic challenges due to the phase-incompatibility of the two tailgroups.[39] Alternatively, by taking advantage of the enhanced stability afforded by the "chelate effect" of aromatic bidentate adsorbates,[50−53] one can generate mixed monolayers that are resistant to displacement and allow for fine-tuning the interfacial properties of a surface.

Herein, we report the first example, to our knowledge, of mixed phase-incompatible surfaces composed of a mixture of fluorocarbons and oligo(ethylene glycol) chains, where the surface concentration mirrors that of the relative concentrations of the adsorbates in the developing solution. The adsorbates used to obtain the mixed surfaces are shown in Figure 1.

(5-((9,9,10,10,11,11,12,12,13,13,14,14,15,15,16,16,16-Heptadecafluorohexadecyl)oxy)-1,3-phenylene)dimethanethiol (PFPDT) and (5-((2,5,8,11-tetraoxahexadecan-16-yl)oxy)-1,3-phenylene)dimethanethiol (OEGPDT) were used. For comparison, the monodentate analogs, 9,9,10,10,11,11,12,12,13,13,14,14,15,15,16,16,16-heptadecafluorohexadecane-1-thiol (PFT) and 2,5,8,11-tetraoxahexadecane-16-thiol (OEGT), were also used to generate reference SAM systems. The interfacial properties of all of the SAMs were characterized using optical ellipsometry, polarization−modulation infrared reflection absorption spectroscopy (PM-IRRAS), X-ray photoelectron spectroscopy (XPS), and contact angle goniometry.

■ EXPERIMENTAL SECTION

Comprehensive details regarding the synthetic procedures, instrumental equipment, and materials and methods used to perform this research are provided as Supporting Information.
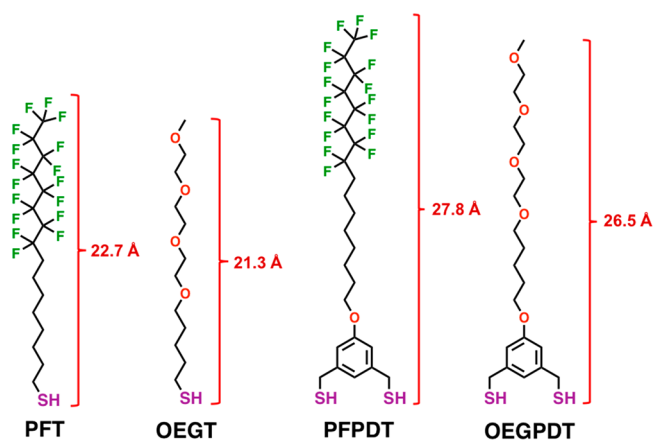

Figure 1. Structure of the monodentate adsorbates, PFT and OEGT, and bidentate adsorbates, PFPDT and OEGPDT, used in the study. The molecular lengths of all adsorbates, assuming fully trans-extended chains, were calculated using ChemBio3D and are provided for reference.

■ RESULTS AND DISCUSSION

The monolayers were generated on freshly evaporated gold surfaces according to the amounts listed in Tables S1 and S2. The nomenclature of the mixed monolayer surfaces is derived from the mole fraction of the fluorinated adsorbate (PFT or PFPDT) in solution; a detailed overview of the mole fraction of each adsorbate present in the mixed SAM solutions is given in Table 1. The total immersion time used to generate the

Table 1. Mole Fraction of Adsorbates in Solution Used to Generate the Mixed SAMs[a]

	mole fraction of adsorbate in solution			mole fraction of adsorbate in solution	
abbreviation	PFT	OEGT	abbreviation	PDPFT	OEGPDT
PFT(1.00)	1.00	0.00	PFPDT(1.00)	1.00	0.00
PFT(0.75)	0.75	0.25	PFPDT(0.75)	0.75	0.25
PFT(0.50)	0.50	0.50	PFPDT(0.50)	0.50	0.50
PFT(0.25)	0.25	0.75	PFPDT(0.25)	0.25	0.75
OEGT(1.00)	0.00	1.00	OEGPDT(1.00)	0.00	1.00

[a]The total adsorbate concentration for both series was maintained at 0.1 mM.

SAMs in this study was 24 h to ensure that equilibrium surface concentrations were reached.[5] Moreover, we chose to evaluate various solvents to determine the conditions needed to generate films with optimal packing and S−Au binding. Prior research has shown that the solvent system used to generate SAMs strongly impacts the adsorbate binding to the surface of gold.[6,46,47] Accordingly, we explored the use of ethanol (EtOH), tetrahydrofuran (THF), N,N-dimethylformamide (DMF), and isooctane to develop the single-component SAMs while maintaining a concentration of 0.1 mM for all adsorbates.

Effect of Developing Solvent on the Formation of Single-Component SAMs. Prior to generating the mixed SAMs, we chose to evaluate and optimize film forming conditions of the individual adsorbates in the monodentate series (PFT and OEGT) and the bidentate series (PFPDT, and OEGPDT). Several solvents ranging in polarity—polar protic, nonpolar aprotic, and polar aprotic—were used to study

the effect of the solvent on the binding of the sulfur of the adsorbates onto the surface of gold. This evaluation was accomplished by analyzing the samples using X-ray photoelectron spectroscopy (XPS); specifically, the binding energy of the S 2p peak in the SAMs was evaluated to determine the amount of bound thiol.[54] Sulfur species in the S 2p region produce peaks with spin−orbital splitting, and the splitting of the peaks is based on the projections of the total angular moments that define the occupancy of the $2p_{1/2}$ and $2p_{3/2}$ levels.[55] An in-depth discussion of the aforementioned phenomenon regarding the S 2p spectra can be found in the literature.[56,57] For sulfur covalently bound to gold, the binding energy of the S $2p_{3/2}$ peak appears at ∼162 eV; in contrast, the binding energy of the S $2p_{3/2}$ peak for an unbound thiol appears at ∼163.5 eV.[7] The binding energy coupled with the ratios of the S 2p peaks allow for an interpretation of the degree of bound vs unbound sulfur species.

The XPS spectra of the S 2p region for the monodentate and bidentate SAMs generated in the tested solvents are shown in Figure 2. For the monodentate series (PFT and OEGT), initial inspection of the S 2p region reveals the presence of bound thiolates for the four tested solvents. To obtain a more qualitative analysis, the percentage of bound thiolate was calculated by deconvoluting the S 2p peaks (Figures S1 and S2) and is summarized in Table 2. For the monodentate SAMs generated in EtOH, THF, and DMF, the PFT and OEGT adsorbates bind to the surface of gold similarly at 100 ± 0% and 90 ± 2%, respectively. There is a slight decrease in the amount of bound thiol to the gold surface when isooctane was used as the developing solvent, 95 ± 3% and 87 ± 4% for the PFT and OEGT adsorbates, respectively. For the monodentate series, since there was no significant difference between EtOH and THF, nor any improvement with the use of DMF and isooctane in the binding of the sulfur, EtOH was chosen as the solvent for the mixed SAMs generated from the monodentate adsorbates.

A similar analysis was performed for the bidentate adsorbates (PFPDT and OEGPDT); the deconvolutions of the S 2p peaks are shown in Figures S3 and S4. For the SAMs generated from both adsorbates, there is a significant amount of unbound sulfur on the gold surface in all tested solvents, Figure 2. Notably, both SAMs developed in DMF and isooctane generated films with the poorest binding, 61% for OEGPDT in DMF, 59% and 57% for the PFPDT and OEGPDT, respectively, in isooctane; deconvolution of the S 2p peak for the PFPDT SAMs generated in DMF was not performed since the sulfur peak in the spectra indicated oxidation of the sulfur along with substantial unbound thiolates, ∼167 eV.[58,59] For the PFPDT SAMs generated in THF, the deconvolution spectra suggest 76% bound thiol. However, analysis of the SAMs obtained from the adsorption of OEGPDT in THF showed no significant improvement over the film obtained in EtOH. Our initial aim was to generate the targeted mixed monolayers using a single solvent; however, on the basis of these observations and the poor solubility of the PFPDT in EtOH, we pursued the use of mixed solvent systems composed of the two best performing solvents, EtOH and THF, in order to generate strongly bound and densely packed films.

The S 2p region for the single-component SAMs generated from PFPDT and OEGPDT in various volume ratios of THF:EtOH (1:0, 3:1, 1:1, 1:3, and 0:1) is shown in Figure S5. The percentage of bound thiolate was also calculated by
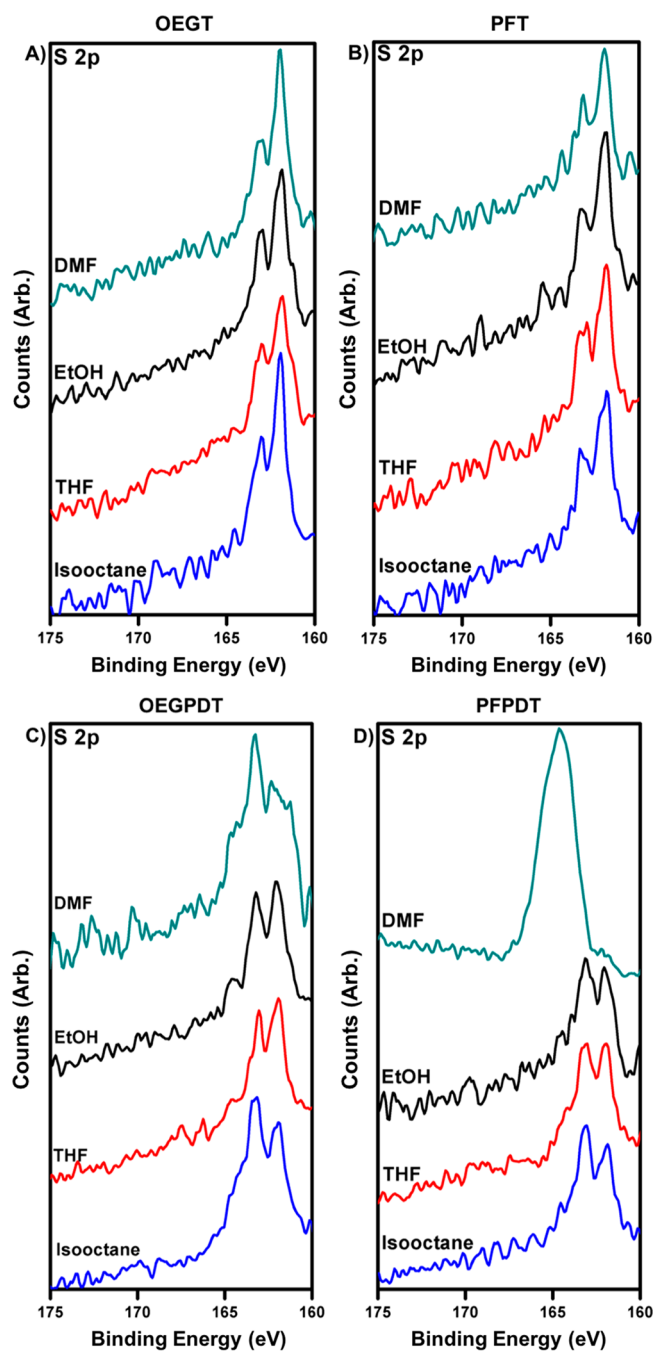

Figure 2. XPS spectra of the S 2p region for the SAMs generated from (A) OEGT, (B) PFT, (C) OEGPDT, and (D) PFPDT in various individual solvents (DMF, EtOH, THF, and isooctane).

Table 2. Percentage of Bound Thiol for the SAMs Generated in Various Solvents[a]

	bound thiol (%)			
adsorbate	ethanol	THF	DMF	isooctane
PFT	100 ± 0	100 ± 0	100 ± 0	95 ± 3
OEGT	93 ± 3	90 ± 2	92 ± 3	87 ± 4
PFPDT	70 ± 4	76 ± 4		59 ± 3
OEGPDT	82 ± 3	78 ± 4	61 ± 4	57 ± 4

[a]Calculations of the percentage of bound thiolate were based on three independent sets of experiments.

deconvolution of the S 2p peaks (Figure S6); the calculated percentages are reported in Table S3. All conditions tested— THF:EtOH (1:3), THF:EtOH (1:1), and THF:EtOH (3:1)— showed similar results in terms of the percentage of bound thiol. Interesting to note is the apparent formation of multilayers as the amount of THF was increased, particularly in the 1:1 and 3:1 samples. Taking all of the results into consideration, we chose to generate mixed SAMs from the monodentate adsorbates (PFT and OEGT) in EtOH, and from the bidentate adsorbates (OEGPDT and PDPFT) in a 1:3 ratio of THF:EtOH.

Characterization by Ellipsometry. The thickness of the SAMs generated from both the monodentate and bidentate adsorbates and selected mixtures were measured using ellipsometry and are presented in Figure 3. The thicknesses
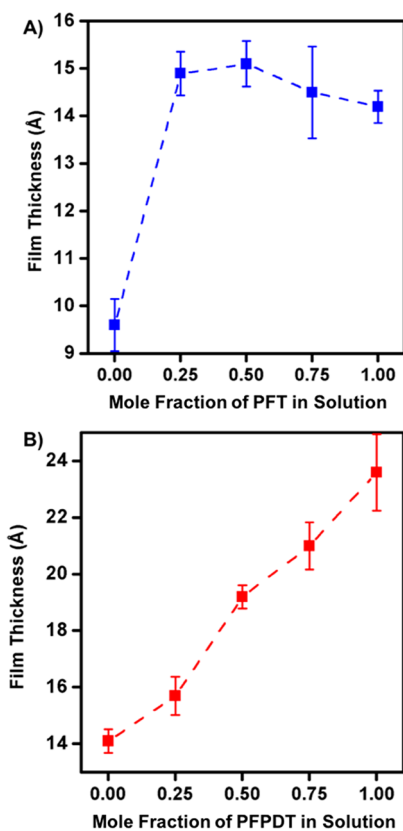

Figure 3. Ellipsometric film thickness for the (A) mixed monodentate SAMs, PFT and OEGT, and (B) mixed bidentate SAMs, PFPDT and OEGPDT. The "0.00" mole fraction represents the single-component SAMs generated from the oligo(ethylene glycol) adsorbate (OEGT and OEGPDT).

of the single-component SAMs were 15, 10, 24, and 15 Å for PFT(1.00), OEGT(1.00), PFPDT(1.00), and OEGPDT(1.00), respectively, and are in accordance with literature values.[53,60−62] As a reference standard, SAMs derived from hexadecanethiol (HDT) exhibited a thickness of 19 Å, which is also consistent with literature values.[60] The bulkiness of the fluorinated moiety of the PFT adsorbate[63] and the flexibility of the oligo(ethylene glycol) moiety of the OEGT adsorbate[64] can lead to films having reduced molecular density compared to the hydrocarbon chain of the HDT and is likely responsible for the lower thicknesses of the former SAMs. Similarly, both PFPDT and OEGPDT, when compared to the

corresponding monodentate adsorbates, possess similar chain lengths and aromatic rings along their backbones; however, the difference in the thickness of the bidentate SAMs, 9 Å (i.e., the difference between PFPDT and OEGPDT SAMs), differs greatly from the difference in thickness of the monodentate SAMs, 5 Å (i.e., the difference between PFT and OEGT SAMs). Apparent from the data, the OEGPDT adsorbate appears to require a larger footprint on the surface than the PFPDT adsorbate, which is consistent with the packing density analysis obtained from the XPS spectra (see Table S10 in the Supporting Information). For the mixed SAMs, one might expect the film thickness to fall somewhere between that of both adsorbates—10−15 Å for the monodentate SAMs, PFT(1.00), and OEGT(1.00) and 15−24 Å for the bidentate SAMs, PFPDT(1.00) and OEGPDT(1.00). However, we found that upon increasing the concentration of PFT in the deposition solution of the monodentate series, the thickness remained constant at around 15 Å. The constant thickness values suggest preferential adsorption of the fluorinated adsorbate, PFT, rather than a mixture of the two adsorbates, which is consistent with an adsorption process that is controlled, at least in part, by thermodynamics. In contrast, upon increasing the concentration of PFPDT in the deposition solution for the bidentate series, we observed a systematic increase in the film thickness. The linear trend observed in the data suggests that PFPDT and OEGPDT adsorb onto the surface with similar probability based on the concentration of the developing solution, which is consistent with an adsorption process that is controlled by kinetics.

Characterization by PM-IRRAS. The PM-IRRAS spectra of the C−H stretching region for the mixed SAMs generated from the monodentate adsorbates (PFT and OEGT), the bidentate adsorbates (PFPDT and OEGPDT), and the reference HDT are provided in Figure 4. The conformational order of the alkyl chains is reflected by the position of the
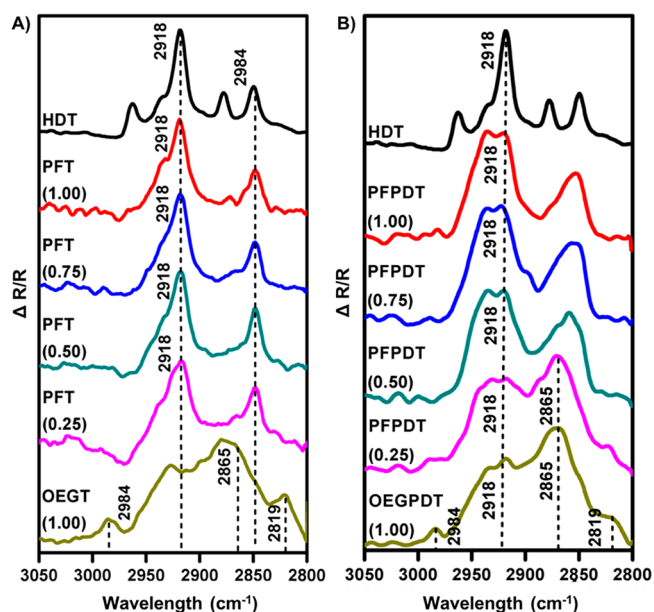

Figure 4. PM-IRRAS spectra of the C−H stretching region for the mixed SAMs generated from (A) the monodentate adsorbates, PFT and OEGT, and (B) the bidentate adsorbates, PFPDT and OEGPDT. Spectra of the SAM generated from HDT are included for comparison.
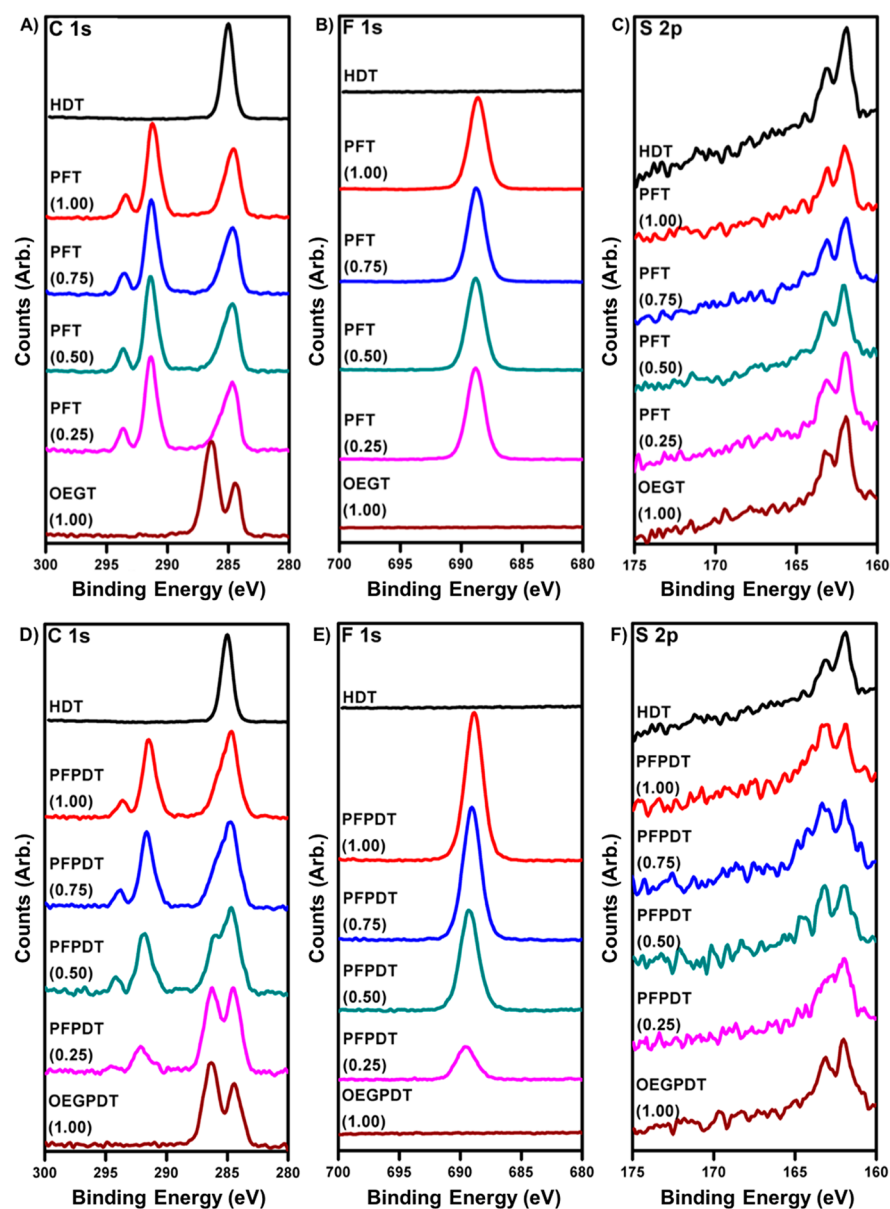
Figure 5. XPS spectra of the (A) C 1s region, (B) F 1s region, and (C) S 2p region for the mixed SAMs generated from the monodentate adsorbates, PFT and OEGT. XPS spectra of the (D) C 1s region, (E) F 1s region, and (F) S 2p region for the mixed SAMs generated between PFPDT and OEGPDT in THF:EtOH (1:3) solution. Spectra of the SAM generated from HDT are included for comparison.

methylene asymmetric ($\nu_{as}^{CH_2}$) and symmetric ($\nu_s^{CH_2}$) stretches. For a conformationally ordered film, such as SAMs generated from long n-alkanethiols, the $\nu_{as}^{CH_2}$ and $\nu_s^{CH_2}$ stretches appear at 2918 and 2849 cm^{-1}, respectively.[60] A shift to longer wavenumber for the $\nu_{as}^{CH_2}$ band indicates a loss of conformational order.[65] Furthermore, the PM-IRRAS spectra can provide additional insight into the composition of the films. The reference SAM generated from HDT exhibited $\nu_{as}^{CH_2}$ and $\nu_s^{CH_2}$ at 2918 and 2850 cm^{-1}, respectively.[65] As shown in Figure 4A for the monodentate adsorbates, the SAM generated solely from the fluorinated adsorbate, PFT(1.00), exhibits stretches associated with only methylene species, $\nu_{as}^{CH_2}$ at 2918 cm^{-1} and $\nu_s^{CH_2}$ at 2848 cm^{-1}, in agreement with the molecular structure of the adsorbate and indicative of a conformationally ordered film. For the SAMs generated solely from the oligo(ethylene glycol) adsorbate, OEGT(1.00), we were unable to draw any conclusions on the

conformational order due to the broadness of the peaks. However, to allow for a rough estimate of the degree of mixing, we assigned the bands that are unique to the OEG group on the basis of literature examples of similarly structured adsorbates (see Table S4).[66] We evaluated the mixed monolayers by focusing on the $\nu_s^{CH_2}$ stretch of the OEG ethylene glycol unit at 2865 cm^{-1}, as well as the $\nu_{as}^{CH_3}$ and $\nu_s^{CH_3}$ stretches of the terminal methoxy OEG ethylene glycol moieties at 2984 and 2819 cm^{-1}, respectively. Apparent from the spectra of the mixed monodentate SAMs, the bands originating from the glycol units fail to appear in the PFT(0.25), PFT(0.50), and PFT(0.75) samples. The absence of these peaks can be interpreted to indicate that the OEGT adsorbate fails to adsorb onto the surface in the presence of the PFT adsorbate, in accordance to the ellipsometry data discussed in the preceding section.

For the SAMs generated from the bidentate adsorbates, a similar analytical approach was taken. The SAM generated solely from the fluorinated adsorbate, PFPDT(1.00), gives rise only to peaks associated with the methylene group, $\nu_{as}^{CH_2}$ and $\nu_{s}^{CH_2}$, at 2918 and 2848 cm^{-1}, respectively, indicating a conformationally ordered film. For the SAM generated solely from the oligo(ethylene glycol) adsorbate, OEGPDT(1.00), peaks corresponding to the glycol units, $\nu_{s}^{CH_2}$, $\nu_{as}^{CH_3}$, and $\nu_{s}^{CH_3}$, were observed at 2869, 2984, and 2819 cm^{-1}, respectively. As for the SAMs derived from OEGT, we were unable to draw any conclusions on the conformational order due to the broadness of the peaks. For the mixed SAMs, overlap between the peaks associated with the glycol units and the alkyl chains of the fluorinated adsorbate further complicate the analysis. Nonetheless, the intensity of the $\nu_{s}^{CH_2}$ of the OEG ethylene glycol unit stretching at 2869 cm^{-1} appears to increase relative to the $\nu_{as}^{CH_2}$ peak of the PFPDT SAM as the concentration of OEGPDT adsorbate is increased. On the basis of the PM-IRRAS spectra, both bidentate adsorbates appear to undergo some degree of mixing on the surface as their concentrations are varied in solution, consistent with the ellipsometry data, whereas, with the monodentate adsorbates, there appears to be preferential adsorption of only the fluorinated adsorbate, PFT. To investigate the composition of the films in a more quantitative manner, we used XPS to characterize the films as described in the following section.

Characterization by XPS. Analysis by XPS provides information on the elemental composition of the surface of interest, with each element in the sample having their own unique binding energy based on their chemical environment.[67] The XPS spectra of the mixed SAMs generated from the monodentate and bidentate adsorbates are shown in Figure 5. For the monodentate SAMs, we begin our analysis of the XPS spectra by examining the SAMs generated from the fluorinated adsorbate PFT(1.00) and the oligo(ethylene glycol)-terminated adsorbate OEGT(1.00) separately. For the PFT(1.00) SAM, the S 2p doublet at ∼161 and ∼162.5 eV confirms the presence of bound thiolate.[7] Furthermore, the XPS spectra of the C 1s region shows the presence of CH$_2$ moieties at ∼285 eV, CF$_2$ at ∼291 eV, and CF$_3$ at ∼293 eV.[11] Additionally, the presence of fluorine is also confirmed by the appearance of a peak in the F 1s region at ∼688 eV. For the OEGT(1.00) SAM, the XPS spectra of the S 2p region confirms the formation of the SAM with a doublet appearing at ∼161 and ∼162.5 eV for S 2p$_{3/2}$ and S 2p$_{1/2}$, respectively. The appearance of a peak ∼287 eV in the C 1s region corresponds to highly oxidized carbon atom (i.e., the carbon atom connected to the oxygen atom in this glycol unit).

Upon mixing the two adsorbates, the spectra of the surface are expected to change to reflect the changes in the relative adsorbate concentration of the solution. For example, as the concentration of the PFT is increased, one might expect the peaks corresponding to the fluorinated components (CF$_2$ and CF$_3$) in the C 1s region as well as the F 1s peak to increase systematically. Correspondingly, a concomitant decrease in the peak intensity corresponding to the OEGT adsorbate (i.e., the C–O component at ∼287 eV), would also be expected. The data for the SAMs derived from the monodentate adsorbates, however, suggest that the fluorinated adsorbate is preferentially adsorbed: the spectra show only peaks associated with CF$_2$ and CF$_3$ (∼291 and ∼293 eV) and no peak for C–O at ∼287 eV. Consequently, the XPS data are in accordance with the film thicknesses and PM-IRRAS spectra discussed in the previous

sections, firmly establishing that the PFT and OEGT adsorbates fail to undergo mixing, which is consistent with a model in which the adsorption process is thermodynamically controlled.

For the mixed SAMs generated from the bidentate adsorbates (PFPDT and OEGPDT), the XPS spectra of the S 2p region show mostly bound thiolates on the gold surface. The C 1s region for the fluorinated bidentate SAM, PFPDT(1.00), shows peaks associated with the CF$_2$ and CF$_3$ carbons at ∼291 and ∼294 eV, respectively, while the saturated carbons (CH$_2$) appear at ∼285 eV, similar to that observed for the PFT(1.00) SAM (vide supra); furthermore, the fluorine atoms also give rise to a peak in the F 1s region at ∼688 eV. The SAMs generated from the oligo(ethylene glycol)-terminated adsorbate, OEGPDT(1.00), show peaks for the CH$_2$ carbons at ∼285 eV and the C–O carbons at ∼287 eV in the C 1s region in the same manner as that observed for the monodentate OEGT(1.00) SAM.

For studies of the SAMs generated from mixtures of the bidentate adsorbates, we monitored the intensities of the peaks unique to the adsorbates: the CF$_2$ and CF$_3$ carbon peaks for the fluorinated adsorbate and the C–O carbon peak for the OEG adsorbate. Apparent from the data, as the concentration of the PFPDT in solution is increased, the intensity of the peaks at ∼291 and ∼294 eV (arising from the CF$_2$ and CF$_3$ carbons, respectively) increases, while the intensity of the peak at ∼287 eV (arising from the C–O carbon) decreases. These results indicate that the oligo(ethylene glycol)-terminated adsorbate (OEGPDT) and the fluorinated adsorbate (PFPDT) co-adsorb to generate mixed SAMs, which is consistent with a model in which the adsorption process is kinetically controlled. To determine precisely how much of each component is present on the surface, a quantitative analysis of both the monodentate and the bidentate systems is provided in the following section.

Quantitative Analysis to Determine the Composition of the Mixed SAMs. We used XPS to determine the precise composition of the mixed SAMs based on the carbon-to-gold (C/Au) and fluorine-to-gold (F/Au) ratios. For all samples, these ratios were obtained from the peak intensities of the Au 1s, C 1s (CF$_2$ peak), and F 1s regions. For the mixed SAMs derived from the monodentate adsorbates, the integrated peak intensities for the calculated ratios (C/Au and F/Au) and relative ratios (C/Au and F/Au) are provided in Table S5, and Figure 6 graphically depicts the relative C/Au and F/Au ratios. For our analysis, the relative C/Au and F/Au ratios of the PFT(1.00) SAM, derived only from the fluorinated adsorbate, were set at 1.00 (100%) and were used as a standard for comparison. Correspondingly, the C/Au and F/Au ratios of the oligo(ethylene glycol)-terminated SAM were set to 0.00. For the PFT(0.25), PFT(0.50), PFT(0.75), and PFT(1.00) SAMs, the relative C/Au ratios (0.99, 0.95, 0.96, and 1.00, respectively) were essentially constant regardless of the solution concentration of the fluorinated adsorbate. A similar trend was observed in the relative F/Au ratios (1.00, 0.99, 0.97, and 1.00, respectively). Both ratios lead to a similar conclusion: the films are composed of largely (if not exclusively) of PFT adsorbates, which is consistent with the previous analyses. For this specific system, the thermodynamic basis for the phenomenon can be attributed to the relative solubility of each adsorbate in ethanol. Empirically, we have observed that the OEGT adsorbate tends to dissolve better in ethanol than the PFT adsorbate; this difference can preferentially drive the
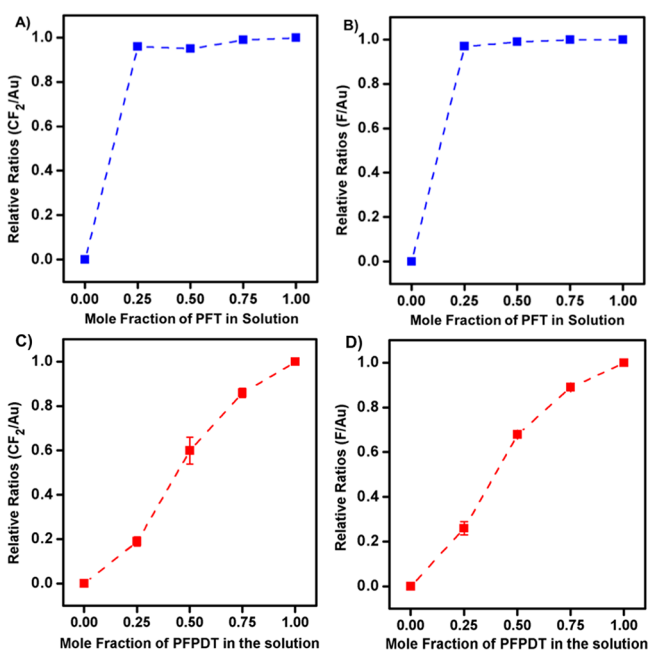
Figure 6. (A) CF$_2$/Au ratio and (B) F/Au ratio of the mixed SAMs generated from monodentate PFT and OEGT in EtOH. (C) CF$_2$/Au ratio and (D) F/Au ratio of the mixed SAMs generated from bidentate PFPDT and OEGPDT in THF:EtOH (1:3).

PFT adsorbate from the solvent and onto the surface of gold. While OEGT can plausibly adsorb simultaneously onto gold, thermondynamically driven displacement of the OEGT adsorbates by PFT adsorbates likely occurs.[53,68]

To evaluate the possible influence of THF when comparing these data to those generated from the bidentate system, we collected the relative C/Au and F/Au ratios for the monodentate system using a 1:3 ratio of THF:EtOH as the developing solution. The data in Table S6 and Figure S7 show the relative C/Au ratios from PFT(0.25), PFT(0.50),

PFT(0.75), and PFT(1.00) SAMs at 0.88, 0.99, 1.00, and, 1.00, respectively. A similar pattern was also observed with the relative F/Au ratios from the PFT(0.25), PFT(0.50), PFT(0.75), and PFT(1.00) SAMs at 0.95, 1.00, 0.99, and, 1.00, respectively. More specifically, a side by side comparison of Tables S5 and S6 as well as Figures 6 and S7 reveals the presence of THF in the 1:3 ratio of THF:EtOH as the developing solution had little or no effect on the molecular composition of the mixed monodentate SAMs. Accordingly, these data confirm the validity of comparing data collected for the monodentate adsorbates PFT and OEGT using EtOH as the developing solution to those collected for the bidentate adsorbates PFPDT and OEGPDT using a 1:3 ratio of THF:EtOH as the developing solution.

To determine the precise composition of the mixed SAMs generated from the bidentate adsorbates, we used the XPS-based approach described above for the monodentate adsorbates. The PFPDT(1.00) SAM was set to have a ratio of 1.00 since the film was composed of pure PFPDT, while the OEGPDT(1.00) film was set to have a ratio of 0.00 since the film was composed of pure OEGPDT adsorbate. The integrated peak intensities for the calculated ratios (C/Au and F/Au) and relative ratios (C/Au and F/Au) are provided in Table S7, and Figure 6 graphically depicts the relative C/Au and F/Au ratios. Additionally, the mole fractions of the mixed SAMs for the monodentate and bidentate adsorbates are shown in Table S8 and Table S9. For the PFPDT(0.25), PFPDT(0.50), and PFPDT(0.75) SAMs, both the CF$_2$/Au and F/Au ratios show a systematic increase in the degree of surface fluorination as the concentration of fluorinated PFPDT in solution is increased. These observations contrast those observed for the SAMs generated from the monodentate adsorbates. The mixing behavior of the bidentate adsorbates can be rationalized on the basis of a kinetic adsorption process that mirrors the solution composition followed by the absence of adsorbate displacement due to the strong binding of the adsorbates to gold via the chelate effect.[53,69] The bidentate adsorbates, PFPDT and OEGPDT, bind to the surface of gold
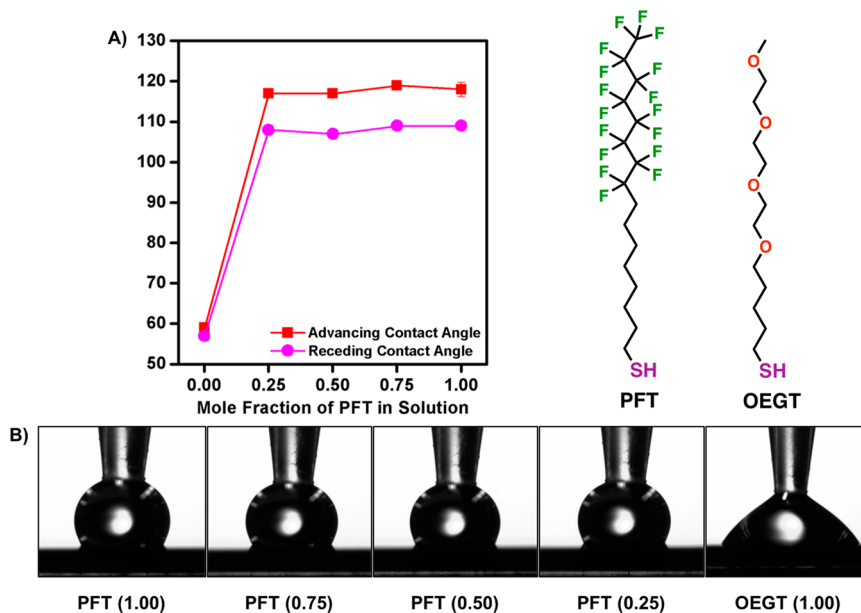

Figure 7. (A) Advancing (red square) and receding (pink square) contact angles of the SAMs. (B) Optical images of the advancing contact angles of water on the mixed SAMs generated from the monodentate adsorbates, PFT and OEGT. Error bars not visible are within the symbol.
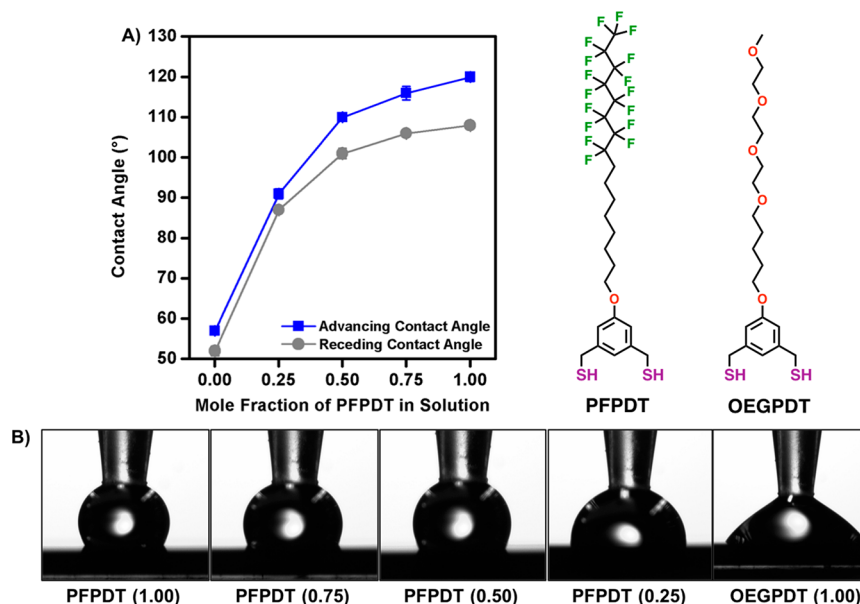
Figure 8. (A) Advancing (blue square) and receding (gray square) contact angles of the SAMs. (B) Optical images of the advancing contact angles of water on the mixed SAMs generated from the bidentate adsorbates, PFPDT and OEGPDT. Error bars not visible are within the symbol.

through two sulfur atoms, which inhibits desorption and thus displacement by adsorbate molecules in solution. In this model, the relative amounts of adsorbates on the surface reflect the relative amounts of the adsorbates in solution. Importantly, these data show that control of the concentration of each adsorbate on the surface can be achieved simply by adjusting the relative solution concentrations of the bidentate adsorbates, allowing facile tuning of the interfacial properties.

Characterization by Contact Angle Goniometry. The advancing and receding contact angles on the mixed SAMs generated from the monodentate and bidentate adsorbates were obtained with water as a probe solvent and are provided in Figures 7 and 8 and summarized in Table S11. Figure 7 shows the advancing and receding contact angles of the mixed monodentate SAMs along with the optical images of the advancing contact angles. The average advancing and receding contact angles of water on the fluorinated PFT(1.00) surface were measured as ∼118° and 107°, respectively, and are in agreement with values measured on other hydrophobic fluorinated films.[27] For the oligo(ethylene glycol)-terminated OEGT(1.00) surface, the advancing and receding contact angles were 59° and 55°, respectively. The lower contact angle compared to the fluorinated SAM, PFT(1.00), can be attributed to the hydrophilicity of the glycol units at the interface, where the oxygen atoms of the ether unit can hydrogen bond with water.[12] Upon increasing the concentration of the PFT adsorbate in the solution, the advancing contact angles remain relatively constant, ∼116 ± 1° (i.e., the contact angles remain unchanged with the addition of OEGT to the solution). These data further support the conclusions presented above: there is preferential/exclusive adsorption of the fluorinated adsorbate (PFT) on the surface for the SAMs generated from the mixtures of the monodentate adsorbates.

The advancing and receding contact angles of water for the mixed SAMs generated from the bidentate PFPDT and OEGPDT adsorbates are shown in Table S11 and Figure 8. The advancing and receding contact angles of the PFPDT(1.00) SAM were 120° and 108°, respectively, and are similar to those measured for the SAM derived from the

monodentate PFT adsorbate. For the OEGPDT SAM, the advancing and receding contact angle values were measured at 57° and 52°, respectively, and are similar to those measured for the SAM derived from the monodentate OEGT SAM. In this series, as the amount of the fluorinated adsorbate was increased, the contact angle also increased. Interestingly, the increases observed in the advancing and receding contact angles do not follow a linear trend as observed with the thickness, PM-IRRAS, and XPS studies. We attribute the nonlinear behavior to the extreme hydrophobicity of the perfluorocarbon tailgroup of the PFPDT adsorbate, which, even at the lowest concentrations studied, disrupts the surface hydration of the neighboring OEG moieties[70] and gives rise to the observed elevated contact angles of water. Furthermore, the nonlinear behavior can be rationalized by the predominantly exposed perfluorocarbons at the SAM−air interface, as indicated by the thicknesses of the single-component PFPDT and OEGPDT films, 24 and 15 Å, respectively.

We note also that the hysteresis values measured for the mixed SAMs generated from the bidentate adsorbates (see Table S11) are similar to the values measured for the single-component SAMs (PFT, OEGT, PFPDT, and OEGPDT). As such, the hysteresis measurements are consistent with a model in which the surface homogeneity and roughness of the mixed bidentate SAMs are comparable to the single-component SAMs. Moreover, these results illustrate that the bidentate adsorbates introduced here can be used to control and selectively tune the interfacial composition such that two strongly phase-incompatible species (fluorocarbon and ethylene glycol tailgroups) coexist as a surface mixture. Future studies will explore the anti-adhesive properties of these unique and unnatural nanomaterials.

■ CONCLUSIONS

Self-assembled monolayers having mixed phase-incompatible tailgroups (fluorocarbon and ethylene glycol) were generated on gold surfaces from solutions containing mixtures of the bidentate adsorbates, PFPDT and OEGPDT. In contrast, solutions containing mixtures of the monodentate analogs,

PFT and OEGT, failed to generate mixtures, instead forming films comprised solely of the perfluorocarbon, PFT. The key driving force for the observed assembly of fluorocarbon and ethylene glycol mixtures was attributed to the "chelate effect" exhibited by the bidentate headgroups of PFPDT and OEGPDT, which bound strongly to the surface of gold and were governed by a kinetically controlled adsorption process. Adsorption of the more weakly bound PFT and OEGT led to films in which the PFT molecules displaced the OEGT molecules to yield thermodynamically controlled surface mixtures comprised of predominantly/exclusively the fluorinated component. Moreover, for the bidentate adsorbates, quantitative analyses revealed that the composition of the adsorbates on the surface closely matched the relative adsorbate percentages used in the developing solution. This first stage of investigation lays the groundwork for generating precisely tuned mixtures of phase-incompatible surface species, which opens new avenues for the creation of unnatural "conflicted" interfaces as nanoscale coatings with exceptional anti-adhesive properties.

■ ASSOCIATED CONTENT

Ⓢ Supporting Information

The Supporting Information is available free of charge at https://pubs.acs.org/doi/10.1021/acsanm.0c00170.

Experimental procedures, including synthetic methods, chemicals, materials, instrumental equipment, characterization techniques, and additional data obtained using PM-IRRAS, XPS, and contact angle goniometry (PDF)

■ AUTHOR INFORMATION

Corresponding Author

T. Randall Lee − Department of Chemistry and the Texas Center for Superconductivity, University of Houston, Houston, Texas 77204-5003, United States; ⓞ orcid.org/0000-0001-9584-8861; Email: trlee@uh.edu

Authors

Siwakorn Sakunkaewkasem − Department of Chemistry and the Texas Center for Superconductivity, University of Houston, Houston, Texas 77204-5003, United States

Maria D. Marquez − Department of Chemistry and the Texas Center for Superconductivity, University of Houston, Houston, Texas 77204-5003, United States

Han Ju Lee − Department of Chemistry and the Texas Center for Superconductivity, University of Houston, Houston, Texas 77204-5003, United States

Complete contact information is available at:
https://pubs.acs.org/10.1021/acsanm.0c00170

Notes

The authors declare no competing financial interest.

■ ACKNOWLEDGMENTS

■ REFERENCES

(1) Abbott, N. L.; Kumar, A.; Whitesides, G. M. Using Micromachining, Molecular Self-Assembly, and Wet Etching to Fabricate 0.1−1-μm-Scale Structures of Gold and Silicon. Chem. Mater. 1994, 6, 596−602.

(2) Nogami, G.; Itagaki, H.; Shiratsuchi, R. Pulsed Electroreduction of CO_2 on Copper Electrodes-II. J. Electrochem. Soc. 1994, 141, 1138−1142.

(3) Sinapi, F.; Forget, L.; Delhalle, J.; Mekhalif, Z. Self-assembly of (3-Mercaptopropyl)Trimethoxysilane on Polycrystalline Zinc Substrates Towards Corrosion Protection. Appl. Surf. Sci. 2003, 212−213, 464−471.

(4) Mrksich, M. Tailored Substrates for Studies of Attached Cell Culture. Cell. Mol. Life Sci. 1998, 54, 653−662.

(5) Mrksich, M. What can Surface Chemistry do for Cell Biology? Curr. Opin. Chem. Biol. 2002, 6, 794−797.

(6) Mrksich, M.; Whitesides, G. M. Using Self-Assembled Monolayers to Understand the Interactions of Man-Made Surfaces with Proteins and Cells. Annu. Rev. Biophys. Biomol. Struct. 1996, 25, 55−78.

(7) Schaeferling, M.; Schiller, S.; Paul, H.; Kruschina, M.; Pavlickova, P.; Meerkamp, M.; Giammasi, C.; Kambhampati, D. Application of Self-Assembly Techniques in the Design of Biocompatible Protein Microarray Surfaces. Electrophoresis 2002, 23, 3097−3105.

(8) Li, Y.; Giesbers, M.; Gerth, M.; Zuilhof, H. Generic Top-Functionalization of Patterned Antifouling Zwitterionic Polymers on Indium Tin Oxide. Langmuir 2012, 28, 12509−12517.

(9) Gleiche, M.; Chi, L. F.; Fuchs, H. Nanoscopic Channel Lattices with Controlled Anisotropic Wetting. Nature 2000, 403, 173−175.

(10) Wilbur, J. L.; Kumar, A.; Biebuyck, H. A.; Kim, E.; Whitesides, G. M. Microcontact Printing of Self-Assembled Monolayers: Applications in Microfabrication. Nanotechnology 1996, 7, 452.

(11) Tan, J. L.; Tien, J.; Chen, C. S. Microcontact Printing of Proteins on Mixed Self-Assembled Monolayers. Langmuir 2002, 18, 519−523.

(12) Tao, F.; Bernasek, S. L. Self-Assembled Monolayers. In Comprehensive Nanoscience and Technology, Vo. 5; Andrews, D. L., Scholes, G. D., Wiederrecht, G. P., Eds.; Academic Press: Amsterdam, 2011; pp 127−152, DOI: 10.1016/B978-0-12-374396-1.00050-7.

(13) Mullen, T. J.; Dameron, A. A.; Weiss, P. S. Directed Assembly and Separation of Self-Assembled Monolayers via Electrochemical Processing. J. Phys. Chem. B 2006, 110, 14410−14417.

(14) Dameron, A. A.; Charles, L. F.; Weiss, P. S. Structures and Displacement of 1-Adamantanethiol Self-Assembled Monolayers on Au{111}. J. Am. Chem. Soc. 2005, 127, 8697−8704.

(15) Miller, M. S.; Juan, R. R. S.; Ferrato, M.-A.; Carmichael, T. B. New Dialkyldithiophosphinic Acid Self-Assembled Monolayers (SAMs): Influence of Gold Substrate Morphology on Adsorbate Binding and SAM Structure. Langmuir 2011, 27, 10019−10026.

(16) Zenasni, O.; Jamison, A. C.; Lee, T. R. The Impact of Fluorination on the Structure and Properties of Self-Assembled Monolayer Films. Soft Matter 2013, 9, 6356−6370.

(17) Lu, H.; Zeysing, D.; Kind, M.; Terfort, A.; Zharnikov, M. Structure of Self-Assembled Monolayers of Partially Fluorinated Alkanethiols with a Fluorocarbon Part of Variable Length on Gold Substrate. J. Phys. Chem. C 2013, 117, 18967−18979.

(18) Schwendel, D.; Dahint, R.; Herrwerth, S.; Schloerholz, M.; Eck, W.; Grunze, M. Temperature Dependence of the Protein Resistance of Poly- and Oligo(Ethylene Glycol)-Terminated Alkanethiolate Monolayers. Langmuir 2001, 17, 5717−5720.

(19) Zhu, B.; Eurell, T.; Gunawan, R.; Leckband, D. Chain-Length Dependence of the Protein and Cell Resistance Of Oligo(Ethylene Glycol)-Terminated Self-Assembled Monolayers on Gold. J. Biomed. Mater. Res. 2001, 56, 406−416.

(20) Kankate, L.; Werner, U.; Turchanin, A.; Gölzhäuser, A.; Großmann, H.; Tampé, R. Protein Resistant Oligo(Ethylene Glycol) Terminated Self-Assembled Monolayers of Thiols on Gold by Vapor Deposition in Vacuum. Biointerphases 2010, 5, 30−36.

(21) Huang, R.; Ferhan, A. R.; Guo, L.; Qiu, B.; Lin, Z.; Kim, D.-H.; Chen, G. In situ Synthesis of Protein-Resistant Poly(Oligo(Ethylene Glycol)Methacrylate) Films in Capillary for Protein Separation. RSC Adv. 2014, 4, 4883−4888.

(22) Vaish, A.; Vanderah, D. J.; Vierling, R.; Crawshaw, F.; Gallagher, D. T.; Walker, M. L. Membrane Protein Resistance of Oligo(Ethylene Oxide) Self-Assembled Monolayers. *Colloids Surf., B* **2014**, *122*, 552−558.

(23) Senaratne, W.; Andruzzi, L.; Ober, C. K. Self-Assembled Monolayers and Polymer Brushes in Biotechnology: Current Applications and Future Perspectives. *Biomacromolecules* **2005**, *6*, 2427−2448.

(24) Krishnan, S.; Weinman, C. J.; Ober, C. K. Advances in Polymers for Anti-Biofouling Surfaces. *J. Mater. Chem.* **2008**, *18*, 3405−3413.

(25) Barriet, D.; Lee, T. R. Fluorinated Self-Assembled Monolayers: Composition, Structure and Interfacial Properties. *Curr. Opin. Colloid Interface Sci.* **2003**, *8*, 236−242.

(26) Colorado, R.; Lee, T. R. Physical Organic Probes of Interfacial Wettability Reveal the importance of Surface Dipole Effects. *J. Phys. Org. Chem.* **2000**, *13*, 796−807.

(27) Colorado, R.; Lee, T. R. Wettabilities of Self-Assembled Monolayers on Gold Generated from Progressively Fluorinated Alkanethiols. *Langmuir* **2003**, *19*, 3288−3296.

(28) Luscombe, C. K.; Li, H.-W.; Huck, W. T. S.; Holmes, A. B. Fluorinated Silane Self-Assembled Monolayers as Resists for Patterning Indium Tin Oxide. *Langmuir* **2003**, *19*, 5273−5278.

(29) Velleman, L.; Shapter, J. G.; Losic, D. Gold Nanotube Membranes Functionalised with Fluorinated Thiols for Selective Molecular Transport. *J. Membr. Sci.* **2009**, *328*, 121−126.

(30) Pale-Grosdemange, C.; Simon, E. S.; Prime, K. L.; Whitesides, G. M. Formation of Self-Assembled Monolayers by chemisorption of derivatives of Oligo(Ethylene Glycol) of Structure HS-$(CH_2)_{11}(OCH_2CH_2)_mOH$ on Gold. *J. Am. Chem. Soc.* **1991**, *113*, 12−20.

(31) Ista, L. K.; Fan, H.; Baca, O.; López, G. P. Attachment of Bacteria to Model Solid Surfaces: Oligo(ethylene glycol) Surfaces Inhibit Bacterial Attachment. *FEMS Microbiol. Lett.* **1996**, *142*, 59−63.

(32) Lokanathan, A. R.; Zhang, S.; Regina, V. R.; Cole, M. A.; Ogaki, R.; Dong, M.; Besenbacher, F.; Meyer, R. L.; Kingshott, P. Mixed Poly(Ethylene Glycol) and Oligo (Ethylene Glycol) Layers on Gold as Nonfouling Surfaces Created by Backfilling. *Biointerphases* **2011**, *6*, 180−188.

(33) Ista, L. K.; López, G. P. Interfacial Tension Analysis of Oligo(Ethylene Glycol)-Terminated Self-Assembled Monolayers and Their Resistance to Bacterial Attachment. *Langmuir* **2012**, *28*, 12844−12850.

(34) Svedhem, S.; Hollander, C.-Å.; Shi, J.; Konradsson, P.; Liedberg, B.; Svensson, S. C. T. Synthesis of a Series of Oligo(Ethylene Glycol)-Terminated Alkanethiol Amides Designed to Address Structure and Stability of Biosensing Interfaces. *J. Org. Chem.* **2001**, *66*, 4494−4503.

(35) Boozer, C.; Ladd, J.; Chen, S.; Yu, Q.; Homola, J.; Jiang, S. DNA Directed Protein Immobilization on Mixed ssDNA/Oligo-(ethylene glycol) Self-Assembled Monolayers for Sensitive Biosensors. *Anal. Chem.* **2004**, *76*, 6967−6972.

(36) Raynor, J. E.; Petrie, T. A.; García, A. J.; Collard, D. M. Controlling Cell Adhesion to Titanium: Functionalization of Poly[Oligo(Ethylene Glycol)Methacrylate] Brushes with Cell-Adhesive Peptides. *Adv. Mater.* **2007**, *19*, 1724−1728.

(37) Dietrich, H.; Scheiner, S.; Portilla, L.; Zahn, D.; Halik, M. Improving the Performance of Organic Thin-Film Transistors by Ion Doping of Ethylene-Glycol-Based Self-Assembled Monolayer Hybrid Dielectrics. *Adv. Mater.* **2015**, *27*, 8023−8027.

(38) Love, J. C.; Estroff, L. A.; Kriebel, J. K.; Nuzzo, R. G.; Whitesides, G. M. Self-Assembled Monolayers of Thiolates on Metals as a Form of Nanotechnology. *Chem. Rev.* **2005**, *105*, 1103−1170.

(39) Marquez, M. D.; Zenasni, O.; Jamison, A. C.; Lee, T. R. Homogeneously Mixed Monolayers: Emergence of Compositionally Conflicted Interfaces. *Langmuir* **2017**, *33*, 8839−8855.

(40) Chapman, R. G.; Ostuni, E.; Yan, L.; Whitesides, G. M. Preparation of Mixed Self-Assembled Monolayers (SAMs) That Resist Adsorption of Proteins Using the Reaction of Amines with a SAM That Presents Interchain Carboxylic Anhydride Groups. *Langmuir* **2000**, *16*, 6927−6936.

(41) Hoffmann, C.; Tovar, G. E. M. Mixed Self-Assembled Monolayers (SAMs) Consisting of Methoxy-Tri(Ethylene Glycol)-Terminated and Alkyl-Terminated Dimethylchlorosilanes Control the Non-Specific Adsorption of Proteins at Oxidic Surfaces. *J. Colloid Interface Sci.* **2006**, *295*, 427−435.

(42) Folkers, J. P.; Laibinis, P. E.; Whitesides, G. M. Self-Assembled Monolayers of Alkanethiols on Gold: Comparisons of Monolayers Containing Mixtures of short- and long-Chain Constituents with Methyl and Hydroxymethyl Terminal Groups. *Langmuir* **1992**, *8*, 1330−1341.

(43) Laibinis, P. E.; Fox, M. A.; Folkers, J. P.; Whitesides, G. M. Comparisons of Self-Assembled Monolayers on Silver and Gold: Mixed Monolayers Derived from $HS(CH_2)_{21}X$ and $HS(CH_2)_{10}Y$ (X, Y = CH_3, CH_2OH) have Similar Properties. *Langmuir* **1991**, *7*, 3167−3173.

(44) Folkers, J. P.; Laibinis, P. E.; Whitesides, G. M.; Deutch, J. Phase Behavior of Two-Component Self-Assembled Monolayers of alkanethiolates on gold. *J. Phys. Chem.* **1994**, *98*, 563−571.

(45) Rittikulsittichai, S.; Park, C. S.; Marquez, M. D.; Jamison, A. C.; Frank, T.; Wu, C.-H.; Wu, J. I.; Lee, T. R. Inhibiting Reductive Elimination as an Intramolecular Disulfide Dramatically Enhances the Thermal Stability of SAMs on Gold Derived from Bidentate Adsorbents. *Langmuir* **2018**, *34*, 6645−6652.

(46) Chinwangso, P.; Lee, H. J.; Jamison, A. C.; Marquez, M. D.; Park, C. S.; Lee, T. R. Structure, Wettability, and Thermal Stability of Organic Thin-Films on Gold Generated from the Molecular Self-Assembly of Unsymmetrical Oligo(Ethylene Glycol) Spiroalkanedithiols. *Langmuir* **2017**, *33*, 1751−1762.

(47) Chinwangso, P.; Lee, H. J.; Lee, T. R. Self-Assembled Monolayers Generated from Unsymmetrical Partially Fluorinated Spiroalkanedithiols. *Langmuir* **2015**, *31*, 13341−13349.

(48) Chinwangso, P.; St. Hill, L. R.; Marquez, M. D.; Lee, T. R. Unsymmetrical Spiroalkanedithiols Having Mixed Fluorinated and Alkyl Tailgroups of Varying Length: Film Structure and Interfacial Properties. *Molecules* **2018**, *23*, 2632−2654.

(49) Xu, S.; Liu, W. Synthesis and Surface Characterization of an Amphiphilic Fluorinated Copolymer via Emulsifier-Free Emulsion Polymerization of RAFT. *J. Fluorine Chem.* **2008**, *129*, 125−130.

(50) Chinwangso, P.; Jamison, A. C.; Lee, T. R. Multidentate Adsorbates for Self-Assembled Monolayer Films. *Acc. Chem. Res.* **2011**, *44*, 511−519.

(51) Lee, H. J.; Jamison, A. C.; Lee, T. R. Boc-Protected ω-Amino Alkanedithiols Provide Chemically and Thermally Stable Amine-Terminated Monolayers on Gold. *Langmuir* **2015**, *31*, 2136−2146.

(52) Lee, H. J.; Jamison, A. C.; Yuan, Y.; Li, C.-H.; Rittikulsittichai, S.; Rusakova, I.; Lee, T. R. Robust Carboxylic Acid-Terminated Organic Thin Films and Nanoparticle Protectants Generated from Bidentate Alkanethiols. *Langmuir* **2013**, *29*, 10432−10439.

(53) Lee, H. J.; Jamison, A. C.; Lee, T. R. Two Are Better than One: Bidentate Adsorbates Offer Precise Control of Interfacial Composition and Properties. *Chem. Mater.* **2016**, *28*, 5356−5364.

(54) Zharnikov, M. High-resolution X-ray photoelectron spectroscopy in studies of self-assembled organic monolayers. *J. Electron Spectrosc. Relat. Phenom.* **2010**, *178*, 380−393.

(55) *Surface Analysis by Auger and X-Ray Photoelectron Spectroscopy*; IM: Chichester, U.K., 2003.

(56) Vickerman, J. C., Gilmore, I. S., Eds. *Surface Analysis—The Principal Techniques*, 2nd ed.; John Wiley and Sons: Chichester, U.K., 2009; DOI: 10.1002/9780470721582.

(57) Castner, D. G.; Hinds, K.; Grainger, D. W. X-ray Photoelectron Spectroscopy Sulfur 2p Study of Organic Thiol and Disulfide Binding Interactions with Gold Surfaces. *Langmuir* **1996**, *12*, 5083−5086.

(58) Vericat, C.; Vela, M. E.; Benitez, G.; Carro, P.; Salvarezza, R. C. Self-Assembled Monolayers of Thiols and Dithiols on Gold: New Challenges for a Well-Known System. *Chem. Soc. Rev.* **2010**, *39*, 1805−1834.

(59) Lee, M.-T.; Hsueh, C.-C.; Freund, M. S.; Ferguson, G. S. Air Oxidation of Self-Assembled Monolayers on Polycrystalline Gold: The Role of the Gold Substrate. *Langmuir* **1998**, *14*, 6419−6423.

(60) Bain, C. D.; Troughton, E. B.; Tao, Y. T.; Evall, J.; Whitesides, G. M.; Nuzzo, R. G. Formation of Monolayer Films by the Spontaneous Assembly of Organic Thiols from Solution onto Gold. *J. Am. Chem. Soc.* **1989**, *111*, 321−335.

(61) Yuan, Y.; Yam, C. M.; Shmakova, O. E.; Colorado, R.; Graupe, M.; Fukushima, H.; Moore, H. J.; Lee, T. R. Solution-Phase Desorption of Self-Assembled Monolayers on Gold Derived From Terminally Perfluorinated Alkanethiols. *J. Phys. Chem. C* **2011**, *115*, 19749−19760.

(62) Zhu, B.; Eurell, T.; Gunawan, R.; Leckband, D. Chain-Length Dependence of the Protein and Cell Resistance of Oligo(Ethylene Glycol)-Terminated Self-Assembled Monolayers on Gold. *J. Biomed. Mater. Res.* **2001**, *56*, 406−416.

(63) Frey, S.; Heister, K.; Zharnikov, M.; Grunze, M.; Tamada, K.; Colorado, R., Jr; Graupe, M.; Shmakova, O. E.; Lee, T. R. Structure of Self-Assembled Monolayers of Semifluorinated Alkanethiols on Gold and Silver Substrates. *Isr. J. Chem.* **2000**, *40*, 81−97.

(64) Yang, R.; Yang, X. R.; Evans, D. F.; Hendrickson, W. A.; Baker, J. Scanning Tunneling Microscopy Images of Poly(Ethylene Oxide) Polymers: Evidence for Helical and Superhelical Structures. *J. Phys. Chem.* **1990**, *94*, 6123−6125.

(65) Porter, M. D.; Bright, T. B.; Allara, D. L.; Chidsey, C. E. D. Spontaneously Organized Molecular Assemblies. 4. Structural Characterization of *n*-Alkyl Thiol Monolayers on Gold by Optical Ellipsometry, Infrared Spectroscopy, and Electrochemistry. *J. Am. Chem. Soc.* **1987**, *109*, 3559−3568.

(66) Harder, P.; Grunze, M.; Dahint, R.; Whitesides, G. M.; Laibinis, P. E. Molecular Conformation in Oligo(Ethylene Glycol)-Terminated Self-Assembled Monolayers on Gold and Silver Surfaces Determines Their Ability To Resist Protein Adsorption. *J. Phys. Chem. B* **1998**, *102*, 426−436.

(67) Laibinis, P. E.; Whitesides, G. M.; Allara, D. L.; Tao, Y. T.; Parikh, A. N.; Nuzzo, R. G. Comparison of the Structures and Wetting Properties of Self-Assembled Monolayers of *n*-Alkanethiols on the Coinage Metal Surfaces, Copper, Silver, and Gold. *J. Am. Chem. Soc.* **1991**, *113*, 7152−7167.

(68) Son, Y. J.; Han, S.; Yoshizawa, K.; Hayashi, T.; Hara, M.; Noh, J. Displacement Processes of 1-Adamanetanethiol Self-Assembled Monolayers on Au(111) by 1-Hexanethiol. *J. Nanosci. Nanotechnol.* **2019**, *19*, 4732−4735.

(69) Martell, A. E. The Chelate Effect. In *Werner Centennial*; American Chemical Society, 1967; Vol. *62*, pp 272−294, DOI: 10.1021/ba-1967-0062.ch019.

(70) Zheng, J.; Li, L.; Tsao, H.-K.; Sheng, Y.-J.; Chen, S.; Jiang, S. Strong Repulsive Forces between Protein and Oligo (Ethylene Glycol) Self-Assembled Monolayers: A Molecular Simulation Study. *Biophys. J.* **2005**, *89*, 158−166.